applied sciences

MDPI

Article

Effect of Magnetic Nanofluids on the Performance of a Fin-Tube Heat Exchanger

Yun-Seok Choi and Youn-Jea Kim *

School of Mechanical Engineering, Sungkyunkwan University, Suwon 16419, Korea; ysc199@skku.edu
* Correspondence: yjkim@skku.edu; Tel.: +82-31-290-7495

Abstract: As electrical devices become smaller, it is essential to maintain operating temperature for safety and durability. Therefore, there are efforts to improve heat transfer performance under various conditions, such as using extended surfaces and nanofluids. Among them, cooling methods using ferrofluid are drawing the attention of many researchers. This fluid can control the movement of the fluid in magnetic fields. In this study, the heat transfer performance of a fin-tube heat exchanger, using ferrofluid as a coolant, was analyzed when external magnetic fields were applied. Permanent magnets were placed outside the heat exchanger. When the magnetic fields were applied, a change in the thermal boundary layer was observed. It also formed vortexes, which affected the formation of flow patterns. The vortex causes energy exchanges in the flow field, activating thermal diffusion and improving heat transfer. A numerical analysis was used to observe the cooling performance of heat exchangers, as the strength and number of the external magnetic fields were varying. VGs (vortex generators) were also installed to create vortex fields. A convective heat transfer coefficient was calculated to determine the heat transfer rate. In addition, the comparative analysis was performed with graphical results using contours of temperature and velocity.

Keywords: ferrofluid; magnetic field; fin-tube heat exchanger; vortex generators; heat transfer

Citation: Choi, Y.-S.; Kim, Y.-J. Effect of Magnetic Nanofluids on the Performance of a Fin-Tube Heat Exchanger. *Appl. Sci.* **2021**, *11*, 9261. https://doi.org/10.3390/app11199261

Academic Editor: Luis Lugo

Received: 9 September 2021
Accepted: 28 September 2021
Published: 6 October 2021

1. Introduction

Heat dissipation is very important because it is directly related to the life and safety of electronic devices. Accordingly, various studies for managing heat in electronic devices are being conducted [1]. Among them, this study aimed to improve the heat transfer performance using ferrofluid. Ferrofluid is a colloidal suspension, containing magnetic nanoparticles with a diameter of 3 to 15 nm [2]. There are many kinds of particles, such as Fe_3O_4, $CoFeO_4$, and FePt, which have ferromagnetic properties. Due to the magnetism of the particles, this fluid has the characteristic of reacting with a magnetic field. When a magnetic field is applied, the fluid has kinetic energy and forms a specific shape [3]. That is, there are the advantages that a flow can be created only by a magnetic force without direct contact with the fluid, and that control is possible with a relatively simple configuration. In addition, it was confirmed that nanofluids have superior thermal performance compared to general fluid, due to the properties of the particles [4,5].

Yamaguchi et al. [6] observed heat transfer by natural convection when a magnetic fluid is contained in a cavity. AR (aspect ratio) values, such as 1, 1.5, and 2 of the cavity, were set as variables. Ra_m (magnetic Rayleigh number), Ra (Rayleigh number), Ra_c (critical Rayleigh number) corresponding to each variable were observed. As AR increased, the Ra_c tended to decrease, and it was confirmed that many vortex fields appeared. In addition, when a magnetic field was applied, the improvement in heat transfer was confirmed. It is due to the occurrence of various vortex shapes and strong circulation.

Selimefendigil et al. [7] observed the flow phenomenon in a partially heated cavity. In their study, Ra, the location of the heat source and the strength and the location of the magnetic field were set as variables. Circulation was related to the strength of a magnet, and was caused by the partial change in susceptibility, according to the temperature gradient.

It was concluded that the change in the circulation shape increases when the value of Ra also increases.

Ghorbani et al. [8] analyzed the heat transfer performance, according to the strength, number, and position of magnets when high-temperature ferrofluid was injected. Five different magnetic field strengths were specified, and magnets were arranged in six places. When the magnetic field was stronger than a certain standard, the cooling performance was proportionally increased. The small circulation was combined to create a big vortex, which circulated the low-temperature ferrofluid to the relatively high-temperature wall. Finally, the position of magnets showed that the heat transfer performance was improved when all magnets were placed near the cold wall and closer to the inlet area.

Bahiraei et al. [9] placed a permanent magnet in the toroidal loop. Thermomagnetic convection characteristics in which circulation occurs depending on the heat source were used. The magnitude of the heat flux from the heat source, the temperature of the heat sink, the position of the magnet, and the strength of the magnetic field were set as variables. It was shown that the ferrofluid in the loop can be cycled continuously without additional energy consumption. In addition, as the temperature difference between the heat source and the heat sink increased, the circulation speed in the loop increased, indicating that the heat transfer performance was improved.

Bahiraei et al. [10] studied the heat transfer performance when two phases (water and Fe_3O_4) exist in a square channel. The density, particle size, and magnetic field strength of the nanofluid were set as variables. As a result, the heat transfer performance improved as the density and the particle size increased. In addition, it was concluded that the circulation of the fluid increases as the magnetic field strength increases.

Zheng et al. [11] studied the plate heat exchanger under a magnetic field, while working fluids, hot water, and cold ferrofluid were used. Positions of magnets were set into six cases, and the position showing the best heat transfer performance was selected. The case where resistance loss and an improvement in heat transfer performance can be achieved at the same time is when the magnet is set vertically. It was confirmed that the pressure drop decreased when the magnets were arranged without overlapping. Finally, the heat transfer performance and pressure drop were considered at the same time. It was concluded that the optimal effect can be obtained when the magnets are placed vertically in a non-overlapping state.

Bezaatpour et al. [12] compared the cooling performance, according to the magnetic flux density in a fin-tube heat exchanger. Five different densities were set as variables. The cooling performance of the tube farthest from the inlet was the lowest among the three tubes. It was also concluded that the change in the flow was greater when the magnetic flux density was strong.

The purpose of this study was to improve cooling performance, by using ferrofluid in the fin-tube heat exchanger when there is a permanent magnet outside. The numerical analysis was carried out in the absence of magnetic fields, and this result was set as a reference model. Based on this, three conditions were set. The first is a case in which a magnetic field was applied to the reference model. Nanofluids responded to the magnetic field and began to create flows in the heat exchanger. The second involved a case where permanent magnets were added. The last case involved installation of VGs (vortex generators). The heat transfer coefficient was used as an output parameter to compare the cooling performance of these cases. It is believed that these research results can be used as a means to improve the heat dissipation performance of the system in a gravity-free environment, where external forces cannot be applied.

2. Model and Process Description

The reference model used in this study is shown in Figure 1. Figure 1a is a 3D fin-tube heat exchanger model, and Figure 1b is an arbitrary cross-section of a 3D model. The permanent magnet was a neodymium magnet. The space set as the inner chamber was for the ferrofluid. Three tubes with a diameter of 0.6 cm were filled with water and arranged

inside the chamber. The distance between them was 1.4 cm (Figure 1h). The distance from the center of the tube to the Figure 1a side was set to 1.5 cm (Figure 1i). The type of ferrofluid used in this study was EFH-1. This liquid uses oil as the base fluid and is composed of Fe_3O_4 particles. The properties for EFH-1 are shown in Table 1. Nanoparticles in EFH-1 generate flow by an external magnetic field. By controlling the flow using a magnetic field, it is possible to move the fluid in various directions. In addition, there is the advantage that a vortex can be generated by changing the strength of the magnet.

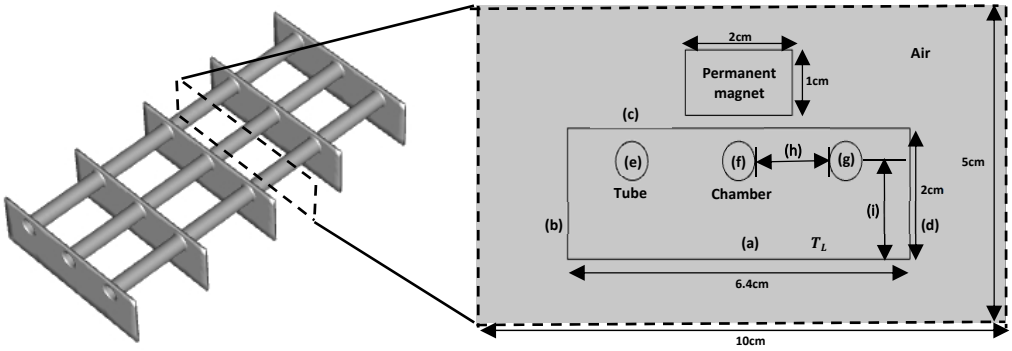

(**a**) (**b**)

Figure 1. Geometry and figures of the reference model applied in this study. (**a**) 3D configuration of a fin-tube heat exchanger model; (**b**) 2D configuration of a fin-tube heat exchanger model.

Table 1. The properties of EFH-1 [13].

Properties	Value
Thermal conductivity	0.19 W/(m·K)
Thermal expansion coefficient	0.00086 1/K
Relative permeability	2.552
Heat capacity at static pressure	1840 J/(kg·K)
Density (T = 298.15 K)	1221 kg/m^3
Dynamic viscosity	0.00727 Pa·s

3. Methodology

3.1. Governing Equations

In this study, numerical analysis was performed using COMSOL Multiphysics, a commercial program for CFD (Computational Fluid Dynamics). Numerical analysis was conducted in a Reynolds-averaged Navier–Stokes (RANS) model, 2D, steady state. Continuity, momentum, and energy equations as the governing equations are as follows [14]:

Continuity:

$$\nabla\cdot\left(\rho\vec{V}\right) = 0 \tag{1}$$

Momentum:

$$\nabla\cdot\left(\rho\vec{V}\vec{V}\right) = -\nabla p + \nabla\cdot\left(\mu\left(\nabla\vec{V} + \left(\nabla\vec{V}\right)^T\right) - \frac{2}{3}\mu\left(\nabla\cdot\vec{V}\right)I + F\right) \tag{2}$$

Energy:

$$\nabla\cdot\left(\vec{V}(\rho E + p)\right) = \nabla\cdot\left(k\nabla T - \sum h_j\vec{J}_j + \left(\overline{\overline{\tau}}\cdot\vec{V}\right)\right) + S_h \tag{3}$$

Since the F term of the momentum equation means the body force due to buoyancy and magnetic force, it has $\rho\beta\left(T - T_{ref}\right)$, which is the body force due to buoyancy, and $\left(\vec{M}\cdot\nabla\right)\vec{B}$,

which is the body force due to magnetic force. Therefore, by substituting two body forces into the momentum Equation (2), the following equation can be finally obtained.

Momentum:

$$\nabla\cdot\left(\rho\vec{V}\vec{V}\right) = -\nabla p + \nabla\cdot(\mu\left(\nabla\vec{V} + \left(\nabla\vec{V}\right)^T\right) - \tfrac{2}{3}\mu\left(\nabla\cdot\vec{V}\right)I + \left(\vec{M}\cdot\nabla\right)\vec{B} + \rho\beta\left(T - T_{ref}\right) \quad (4)$$

Magnetic flux density, B, and magnetic field strength, H, related to Maxwell's equation, are defined as below [15]:

$$\vec{\nabla}\cdot\vec{\mathrm{B}} = 0 \quad (5)$$

$$\vec{\nabla}\times\vec{\mathrm{H}} = 0 \quad (6)$$

Additionally, B can be used to express Gauss's law as follows:

$$\vec{\mathrm{B}} = \mu_0\left(\vec{\mathrm{M}} + \vec{\mathrm{H}}\right) \quad (7)$$

Here, $\mu_0\left(= 4\pi\times10^{-7}\right)$ is a constant value, permeability in a vacuum, and M is magnetization with a unit of A/m.

$$\mathrm{M} = \chi_m\vec{\mathrm{H}} \quad (8)$$

Here, χ_m is magnetic susceptibility, and is defined as follows [16]:

$$\chi_m = \frac{\chi_0}{1+\beta(\mathrm{T}-\mathrm{T}_0)} \quad (9)$$

Here, β and χ_m are the thermal expansion coefficient and magnetic susceptibility at a reference temperature, respectively. From Equation (9), it is shown that χ_m and T are inversely proportional. The convection phenomenon using this property is thermomagnetic convection.

3.2. Grid Systems

Starting with about 100,000 elements, the grid dependence test was conducted a total of 6 times at intervals of about 100,000 elements (Figure 2). The Y-axis uses the total heat flux, q'', and the convergence was confirmed at about 400,000 elements. Therefore, this analysis was conducted at this condition.

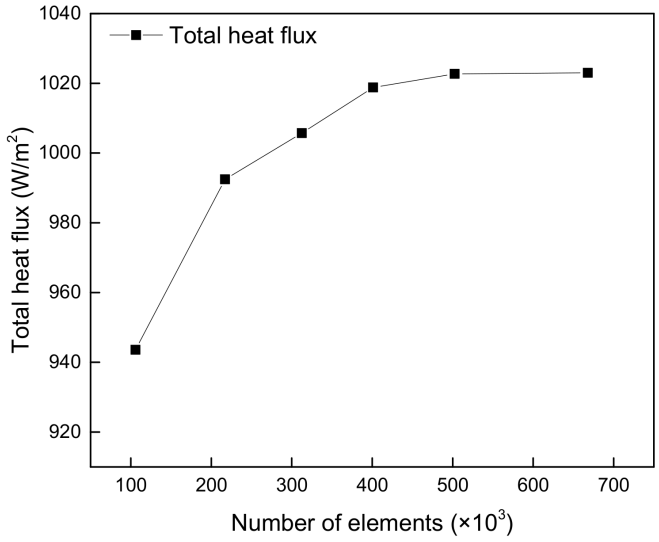

Figure 2. Grid dependency test.

Figure 3 shows partial meshes among the overall shape. The reference model is a simple 2D shape where circular tubes exist and triangular mesh was used. In Figure 3, the mesh densities are different between tubes and the other regions and confirm the flow around the tubes in more detail.

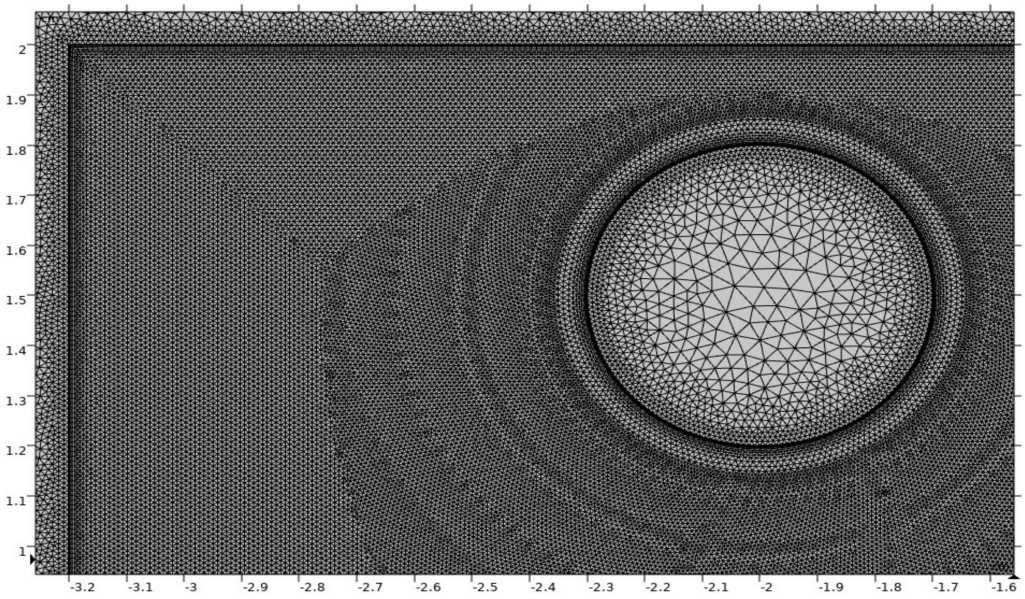

Figure 3. Mesh configurations.

3.3. Boundary Conditions

The boundary conditions are shown in Table 2. The side corresponding to Figure 1a was set as T_L (=288.15 K). The temperature change in the tube surface was observed by setting a heat source of 650 kW/m^3 to the tube. Figure 1b–d include insulation conditions, and a no-slip condition was set for the wall. Numerical analysis was performed by increasing the magnetization value at intervals of 6.0×10^6 A/m based on 6.0×10^6 A/m (Table 3).

Table 2. Boundary conditions applied in this study.

Properties	Value
Heat source	650 kW/m^3
Low temperature (T_L)	288.15 K
Reference temperature	298.15 K
Figure 1b–d boundaries	Adiabatic condition
Wall conditions	No-slip condition

Table 3. Magnetization applied in this study.

Case	Value
Case 1	6.0×10^6 A/m
Case 2	1.2×10^7 A/m
Case 3	1.8×10^7 A/m
Case 4	2.4×10^7 A/m

4. Results and Discussion

To analyze the heat transfer performance of ferrofluid, numerical analysis was performed for four cases, as shown in Figure 4. The case where there was no magnetic field was set as the reference model (Case A). Based on this, the case where there was only one permanent magnet (Case B), the case with three permanent magnets (Case C), and the case

where rectangular VGs for making vortexes were installed (Case D) were compared and analyzed.

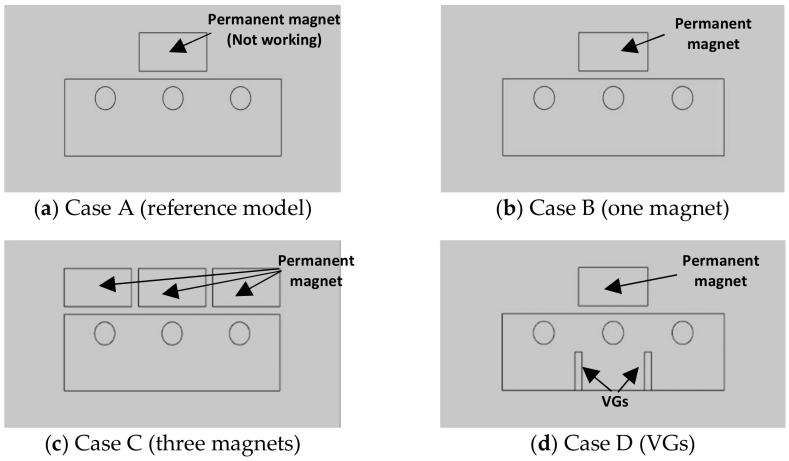

(**a**) Case A (reference model) (**b**) Case B (one magnet)

(**c**) Case C (three magnets) (**d**) Case D (VGs)

Figure 4. Case classification applied in this study.

4.1. Effect of One Permanent Magnet on Heat Transfer

Numerical analysis was performed for the case in which no magnetic field was applied. Figure 5a,b are the velocity and temperature contour results, respectively. Since it is not affected by the magnetic field, the flow velocity was very low. Additionally, looking at the temperature contour, cooling did not occur sufficiently around the tubes. To compare the cooling performance according to the strength of the magnetic field, numerical analysis was performed for four cases. The intensity of magnetization was increased at the same intervals from 6.0×10^6 A/m to 2.4×10^7 A/m.

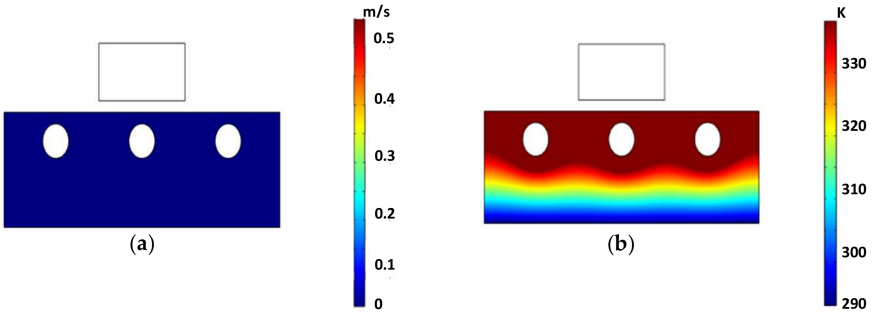

(**a**) (**b**)

Figure 5. Contours of the reference model: (**a**) velocity contour, (**b**) temperature contour.

Because ferrofluid has kinetic energy in magnetic fields, flows began to change, as shown in Figure 6. When compared to the initial magnetization of Figure 6 with Figure 5a, a change in the velocity field was confirmed. As the magnetization value increased, ferrofluid reacted more actively due to nanoparticles. Because the low-temperature ferrofluid near Figure 1a region rose toward a permanent magnet, this fluid pushed the high-temperature ferrofluid near the magnet. Therefore, the circulation shape is clearly visible. Through circulation, the low-temperature ferrofluid at Figure 1a can reach the area (c). In the case of 2.4×10^7 A/m, the most distinct circulation occurred. Therefore, a small vortex was additionally generated in the tube (f).

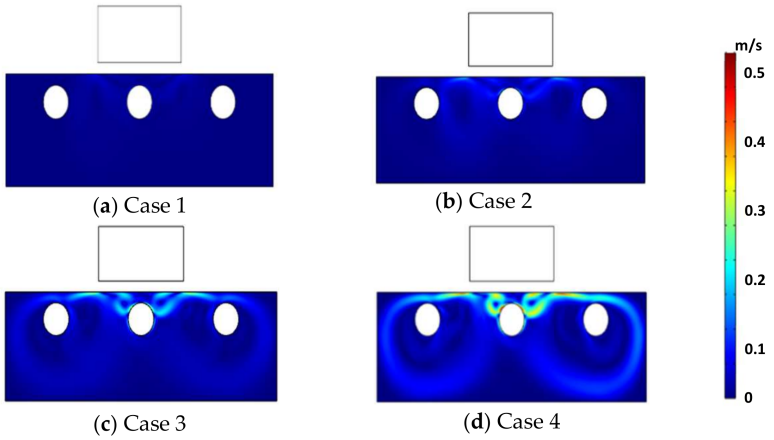

Figure 6. Velocity contours in the case of one permanent magnet (Case B).

In Case 4 of Case B, mixing was most actively performed, and this case shows the best cooling performance among the four cases, as shown in Table 4. When the magnetization value was increased based on 1.8×10^7 A/m, the temperature contour gradually started to change as shown in Figure 7. However, three tubes showed results to suggest that cooling was not happening equally. Temperatures decreased mainly at the Figure 1f tube section. Circulation only affected the tube corresponding to the restricted area, where one permanent magnet was arranged. Additionally, there were stagnation flows at the edge of the chamber. These are factors that deteriorate heat transfer performance.

Table 4. Temperature values in the case of one permanent magnet (Case B).

Case	T_s (K)	T_m (K)
Case 1 $(6.0 \times 10^6$ A/m$)$	352.18	324.68
Case 2 $(1.2 \times 10^7$ A/m$)$	343.35	320.14
Case 3 $(1.8 \times 10^7$ A/m$)$	334.11	315.42
Case 4 $(2.4 \times 10^7$ A/m$)$	326.34	311.47

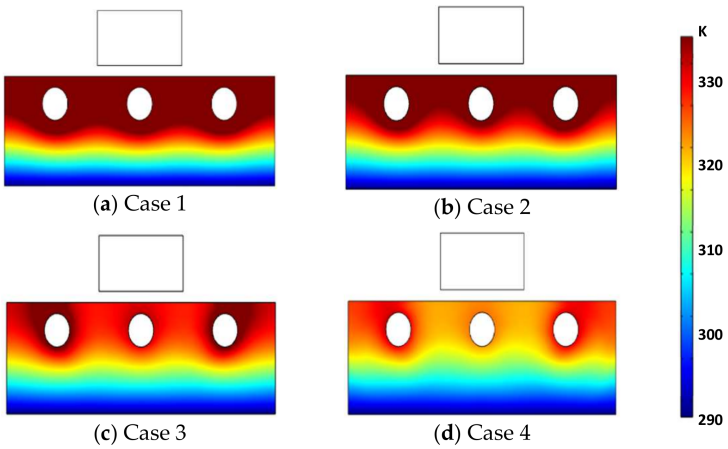

Figure 7. Temperature contours in the case of one permanent magnet (Case B).

4.2. Effect of Three Permanent Magnets on Heat Transfer

To solve the problem of the temperature difference between tubes and stagnation flows, two additional permanent magnets were added. When compared to Case B, several vortexes were made over the entire chamber, including the edges (Figure 8). This means that the heat transfer between the Figure 1a region and tubes was more active, and kinetic energy loss was reduced. This effect can be seen in Case 2 of Figure 9. Unlike Figure 7, which shows cooling at 1.8×10^7 A/m, it is confirmed that cooling was already in progress

at 1.2×10^7 A/m. As the strength of magnetization increased, even cooling proceeded between the three tubes. T_s(K), which represents the surface temperature of the tube, also decreased by about 3.5 °C based on 2.4×10^7 A/m when compared with Tables 4 and 5.

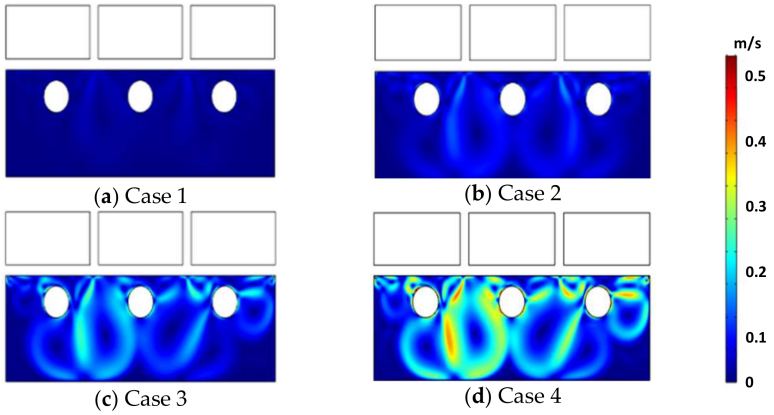

Figure 8. Velocity contours in the case of three permanent magnets (Case C).

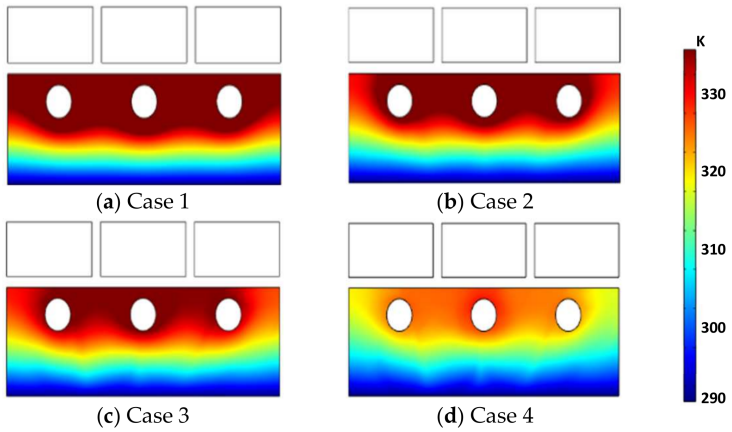

Figure 9. Temperature contours in the case of three permanent magnets (Case C).

Table 5. Temperature values in the case of three permanent magnets (Case C).

Case	T_s (K)	T_m (K)
Case 1 $(6.0 \times 10^6$ A/m)	352.39	325.20
Case 2 $(1.2 \times 10^7$ A/m)	340.45	318.94
Case 3 $(1.8 \times 10^7$ A/m)	333.96	316.23
Case 4 $(2.4 \times 10^7$ A/m)	322.86	309.90

As a result of arranging three permanent magnets, the heat transfer performance was improved by solving the temperature non-uniformity. Although the cooling performance was improved, the efficiency was decreased because of the addition of external permanent magnets.

4.3. Effect of Two VGs on Heat Transfer

To compensate for the shortcomings of installing three permanent magnets, two VGs were placed in the chamber. VGs were installed at the Figure 1a region, where several vortexes combined and the flow velocity was the fastest in Case C. Due to VGs, the highest velocity flow occurred between them (Figure 10). This had the effect of activating the heat exchange between the three tubes, resulting in a uniform cooling effect (Figure 11). In addition, it improved the heat transfer performance by using extended surfaces [17,18]. Based on 2.4×10^7 A/m, T_s of Case D was 321.59 K as shown in Table 6, which had a greater

cooling effect than Cases B and C. By installing just two VGs without additional power, the best cooling performance result was obtained. The convective heat transfer coefficient (h) according to each condition is shown in Figure 12. In the initial magnetization, there was no significant difference in the coefficient between three cases. However, at 2.4×10^7 A/m, the coefficient of Case D increased by 15.5% and 12.6%, respectively, compared to Cases B and C. Nu (Nusselt number) variations for Re (Raynolds number) for all cases are shown in Figure 13. Nu is a parameter that indicates the influence of convection. Comparing Case B and C, Case C had a higher Re at the same magnetization. However, Nu was 1.947 for Case B and 2.014 for Case C based on 2.4×10^7 A/m magnetization. Because it just shows an error of about 3.3%, the influence of convection is similar in both cases. However, Nu of Case D is 2.305, which is about 13–15% higher than that of the other two cases. Convection occurs most actively at Case D. As a result, it can be numerically confirmed that the heat transfer and cooling performance is best achieved by adding VGs.

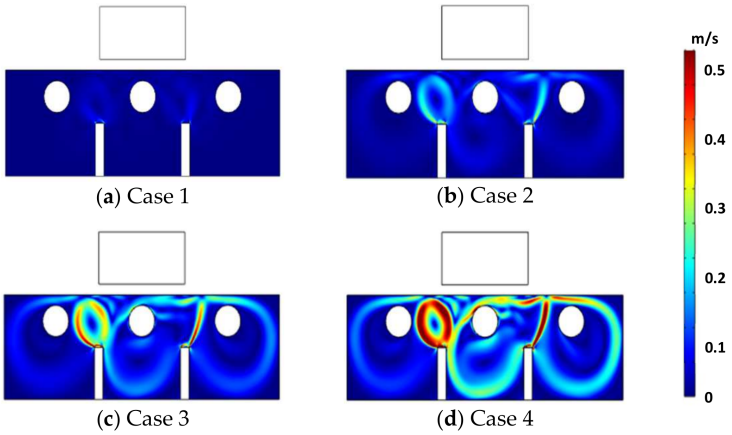

Figure 10. Velocity contours in the case of VGs (Case D).

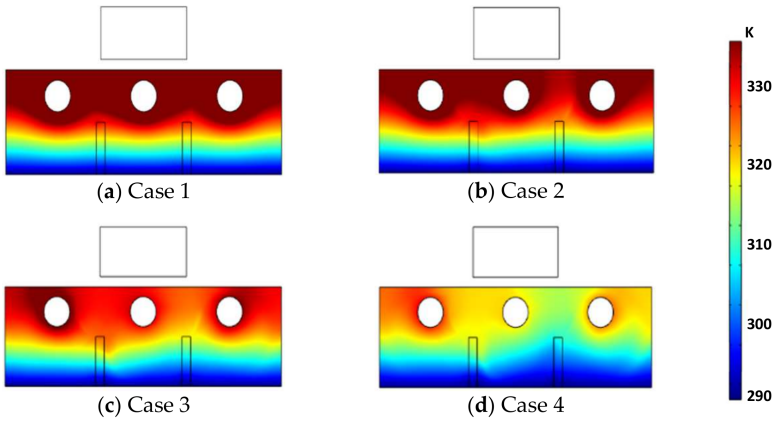

Figure 11. Temperature contours in the case of two VGs (Case D).

Table 6. Temperature values in the case of two VGs (Case D).

Case	T_s (K)	T_m (K)
Case 1 $(6.0 \times 10^6$ A/m$)$	350.58	324.09
Case 2 $(1.2 \times 10^7$ A/m$)$	341.33	319.74
Case 3 $(1.8 \times 10^7$ A/m$)$	332.24	315.37
Case 4 $(2.4 \times 10^7$ A/m$)$	321.59	309.04

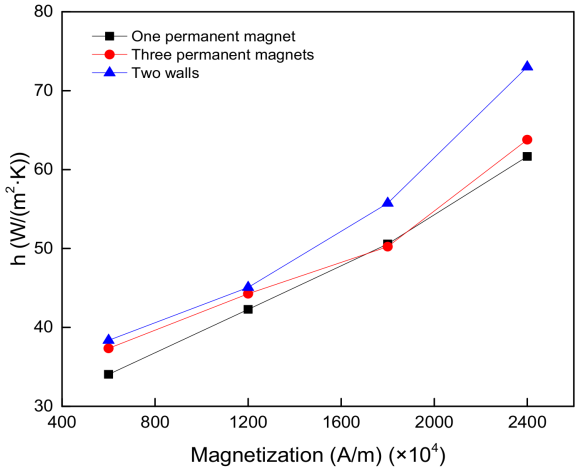

Figure 12. Convective heat transfer coefficient at three cases.

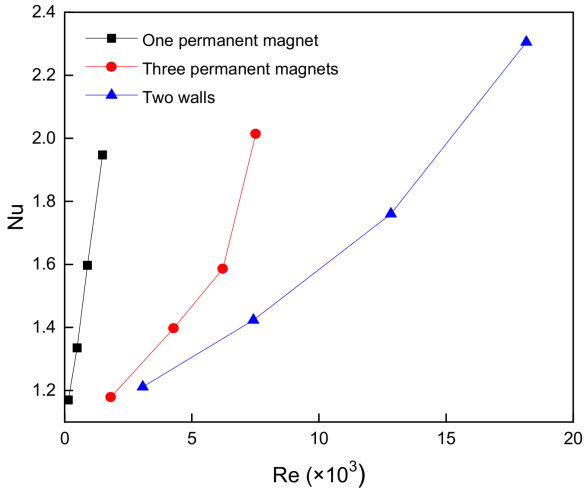

Figure 13. Nusselt number variations for Reynolds number at three cases.

Entropy, shown in Figure 14, is a parameter indicating the state of disorder [19]. Based on prior results, the cooling performance was the best at Case D, and the temperature difference between the heat source and T_L was the smallest. Therefore, the entropy is the smallest at Case D.

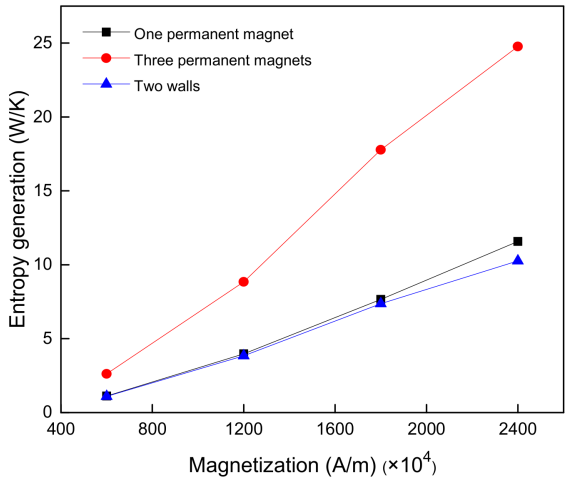

Figure 14. Entropy generation for magnetization at three cases.

5. Conclusions

In this study, the cooling performance of the fin-tube heat exchanger was compared and analyzed under various conditions. In this process, the property of ferrofluid, in which flow is generated by magnetic fields, was used.

- In case B, C, and D, heat transfer and cooling performance were improved by thermal diffusion when the value of magnetization increased.
- When a permanent magnet was applied to the reference model, circulation began to appear around tubes. The low-temperature ferrofluid moved to the Figure 1c area and heat exchange with tubes occurred. However, the uniform cooling effect was not achieved between tubes. Additionally, stagnation flows were confirmed at the edges of the chamber. As a result, there was the disadvantage that cooling was concentrated only at the Figure 1f tube by a permanent magnet.
- To create the uniform cooling effect, permanent magnets of the same size were additionally placed above each tube (Case C). Compared with Case B, a similar temperature distribution was obtained with three tubes. Additionally, vortexes near the edges of the chamber were formed. As a result, the surface temperature was lowered and the mixing effect in the chamber increased.
- By installing VGs in the chamber (Case D), h was improved by 15.6% and 12.6% compared to Cases B and C, respectively, which is a meaningful result. Just by installing VGs at the specific area where several vortexes meet, relatively high-velocity flow regions were formed near the VGs. In addition, the contact areas of the chamber increased as much as the surfaces of VGs. As a result, heat transfer performance improved without additional power supplies.

Author Contributions: Conceptualization, Y.-S.C.; Methodology, Y.-S.C.; Software, Y.-S.C.; Validation, Y.-S.C.; Formal analysis, Y.-S.C.; Investigation, Y.-S.C.; Resources, Y.-S.C.; Data curation, Y.-S.C.; Writing—original draft preparation, Y.-S.C.; Writing—review and editing, Y.-S.C.; Visualization, Y.-S.C.; Supervision, Y.-J.K.; Project administration, Y.-J.K.; Funding acquisition, Y.-J.K. All authors have read and agreed to the published version of the manuscript.

Funding: This research was funded by the National Research Foundation of Korea (NRF), grant number (No. NRF-2021R1A2C1010499).

Institutional Review Board Statement: Not applicable.

Informed Consent Statement: Not applicable.

Data Availability Statement: Not applicable.

Acknowledgments: This work was supported by the National Research Foundation of Korea (NRF), grant funded by the Korea government (MSIT) (No. NRF-2021R1A2C1010499).

Conflicts of Interest: The authors declare no conflict of interest.

References

1. Colangelo, G.; Favale, E.; Milanese, M.; De Risi, A.; Laforgia, D. Cooling of electronic devices: Nanofluids contribution. *Appl. Therm. Eng.* **2017**, *127*, 421–435. [CrossRef]
2. Ellahi, R.; Tariq, M.H.; Hassan, M.; Vafai, K. On boundary layer nano-ferroliquid flow under the influence of low oscillating stretchable rotating disk. *J. Mol. Liq.* **2017**, *229*, 339–345. [CrossRef]
3. Sheikhnejad, Y.; Hosseini, R.; Avval, M.S. Experimental study on heat transfer enhancement of laminar ferrofluid flow in horizontal tube partially filled porous media under fixed parallel magnet bars. *J. Magn. Magn. Mater.* **2017**, *424*, 16–25. [CrossRef]
4. Kristiawan, B.; Santoso, B.; Wijayanta, A.T.; Aziz, M.; Miyazaki, T. Heat transfer enhancement of TiO_2/water nanofluid at laminar and turbulent flows: A numerical approach for evaluating the effect of nanoparticle loadings. *Energies* **2018**, *11*, 1584. [CrossRef]
5. Kristiawan, B.; Wijayanta, A.T.; Enoki, K.; Miyazaki, T.; Aziz, M. Heat transfer enhancement of TiO2/water nanofluids flowing inside a square minichannel with a microfin structure: A numerical investigation. *Energies* **2019**, *12*, 3041. [CrossRef]
6. Yamaguchi, H.; Kobori, I.; Uehata, Y. Heat transfer in natural convection of magnetic fluids. *J.Phys. Heat Transf.* **1999**, *13*, 501–507. [CrossRef]
7. Selimefendigil, F.; Öztop, H.F.; Al-Salem, K. Natural convection of ferrofluids in partially heated square enclosures. *J. Magn. Magn. Mater.* **2014**, *372*, 122–133. [CrossRef]

8. Ghorbani, B.; Ebrahimi, S.; Vijayaraghavan, K. CFD modeling and sensitivity analysis of heat transfer enhancement of a ferrofluid flow in the presence of a magnetic field. *Int. J. Heat Mass Transf.* **2018**, *127*, 544–552. [CrossRef]
9. Bahiraei, M.; Hangi, M. Automatic cooling by means of thermomagnetic phenomenon of magnetic nanofluid in a toroidal loop. *Appl. Therm. Eng.* **2016**, *107*, 700–708. [CrossRef]
10. Bahiraei, M.; Hangi, M.; Rahbari, A. A two-phase simulation of convective heat transfer characteristics of water–Fe_3O_4 ferrofluid in a square channel under the effect of permanent magnet. *Appl. Therm. Eng.* **2019**, *147*, 991–997. [CrossRef]
11. Zheng, D.; Yang, J.; Wang, J.; Kabelac, S.; Sundén, B. Analyses of thermal performance and pressure drop in a plate heat exchanger filled with ferrofluids under a magnetic field. *Fuel* **2021**, *293*, 120432. [CrossRef]
12. Bezaatpour, M.; Rostamzadeh, H. Heat transfer enhancement of a fin-and-tube compact heat exchanger by employing magnetite ferrofluid flow and an external magnetic field. *Appl. Therm. Eng.* **2020**, *164*, 114462. [CrossRef]
13. Kim, J.H.; Seo, H.S.; Kim, Y.J. Thermal-flow characteristics of ferrofluids in a rotating eccentric cylinder under external magnetic force. *Micromachines* **2018**, *9*, 457. [CrossRef] [PubMed]
14. Sheikholeslami, M.; Gerdroodbary, M.B.; Mousavi, S.V.; Ganji, D.D.; Moradi, R. Heat transfer enhancement of ferrofluid inside an 90 elbow channel by non-uniform magnetic field. *J. Magn. Magn. Mater.* **2018**, *460*, 302–311. [CrossRef]
15. Szabo, P.S.; Früh, W.G. The transition from natural convection to thermomagnetic convection of a magnetic fluid in a non-uniform magnetic field. *J. Magn. Magn. Mater.* **2018**, *447*, 116–123. [CrossRef]
16. Bezaatpour, M.; Goharkhah, M. Convective heat transfer enhancement in a double pipe mini heat exchanger by magnetic field induced swirling flow. *Appl. Therm. Eng.* **2020**, *167*, 114801. [CrossRef]
17. Wijayanta, A.T.; Aziz, M.; Kariya, K.; Miyara, A. Numerical study of heat transfer enhancement of internal flow using double-sided delta-winglet tape insert. *Energies* **2018**, *11*, 3170. [CrossRef]
18. Wijayanta, A.T.; Mirmanto; Aziz, M. Heat transfer augmentation of internal flow using twisted tape insert in turbulent flow. *Heat Transf. Eng.* **2020**, *41*, 1288–1300. [CrossRef]
19. Shafee, A.; Haq, R.U.; Sheikholeslami, M.; Herki, J.A.A.; Nguyen, T.K. An entropy generation analysis for MHD water based Fe_3O_4 ferrofluid through a porous semi annulus cavity via CVFEM. *Int. Commun. Heat Mass Transf.* **2019**, *108*, 104295. [CrossRef]